ACS APPLIED MATERIALS & INTERFACES

Subscriber access provided by UNIV OF DURHAM

Biological and Medical Applications of Materials and Interfaces

Fluorescence Resonance Energy Transfer Based Wash-Free Bacterial Imaging and Antibacterial Application Using Cationic Conjugated Polyelectrolyte

Nehal Zehra, Deepanjalee Dutta, Akhtar Hussain Malik,
Siddhartha Sankar Ghosh, and Parameswar Krishnan Iyer

ACS Appl. Mater. Interfaces, **Just Accepted Manuscript** • Publication Date (Web): 27 Jul 2018

Downloaded from http://pubs.acs.org on July 27, 2018

Just Accepted

"Just Accepted" manuscripts have been peer-reviewed and accepted for publication. They are posted online prior to technical editing, formatting for publication and author proofing. The American Chemical Society provides "Just Accepted" as a service to the research community to expedite the dissemination of scientific material as soon as possible after acceptance. "Just Accepted" manuscripts appear in full in PDF format accompanied by an HTML abstract. "Just Accepted" manuscripts have been fully peer reviewed, but should not be considered the official version of record. They are citable by the Digital Object Identifier (DOI®). "Just Accepted" is an optional service offered to authors. Therefore, the "Just Accepted" Web site may not include all articles that will be published in the journal. After a manuscript is technically edited and formatted, it will be removed from the "Just Accepted" Web site and published as an ASAP article. Note that technical editing may introduce minor changes to the manuscript text and/or graphics which could affect content, and all legal disclaimers and ethical guidelines that apply to the journal pertain. ACS cannot be held responsible for errors or consequences arising from the use of information contained in these "Just Accepted" manuscripts.

ACS Publications

is published by the American Chemical Society. 1155 Sixteenth Street N.W., Washington, DC 20036

Published by American Chemical Society. Copyright © American Chemical Society. However, no copyright claim is made to original U.S. Government works, or works produced by employees of any Commonwealth realm Crown government in the course of their duties.

Fluorescence Resonance Energy Transfer Based Wash-Free Bacterial Imaging and Antibacterial Application Using Cationic Conjugated Polyelectrolyte

Nehal Zehra,[1] Deepanjalee Dutta,[2] Akhtar Hussain Malik,[1] Siddhartha Sankar Ghosh,[2,3] and Parameswar Krishnan Iyer*[1,2]*

[1]Department of Chemistry, [2]Centre for Nanotechnology, [3]Department of Biosciences and Bioengineering, Indian Institute of Technology Guwahati, Guwahati 781039, Assam, India.

E-Mail: pki@iitg.ac.in, sghosh@iitg.ac.in

KEYWORDS

Conjugated polyelectrolyte; aggregation induced FRET; ratiometric; biosensor; antibacterial; wash free imaging; fluorescence; cytotoxicity.

ABSTRACT

The increase in bacterial infection and antibiotic resistance has posed a severe threat to the human health. This threat has warranted an imperative demand for the development of new and effective bactericidal material to eradicate the antibiotic-resistant pathogenic bacteria. In this work, we report the wash free imaging of *Staphylococcus aureus* (Gram-positive) and *Escherichia coli* (Gram-negative) bacteria using cationic conjugated polyelectrolyte[9,9-bis(6′-methylimidazoliumbromide)hexyl)-fluorene-co-4,7-(2,1,3 benzothiadiazole)] (PFBT-MI) based on aggregation-induced fluorescence resonance energy transfer (FRET). Cationic imidazolium group strapped on the polymer side chain not only increases its solubility in water but also helps in binding with the negatively charged bacterial membrane via electrostatic interactions to turn on its bright yellow emission. The change in the fluorescence color of conjugated polyelectrolyte in presence of bacteria could be visualized very easily via naked eyes under a UV lamp (365 nm). Furthermore, the antibacterial activity of PFBT-MI against both *Staphylococcus aureus* as well as *Escherichia coli* was observed because of the amphiphilic nature of the conjugated polyelectrolyte which in turn is due to the presence of ionic functionality and conjugated polymer backbone that can intercalate very proficiently into the bacterial membrane, which disrupts the membrane integrity and thus results in toxicity. Morphologically, the membrane damage was perceived via FESEM images, which clearly indicated the disruption of cell membrane upon exposure to PFBT-MI. The PFBT-MI

acts as an effective antibacterial agent, with an MIC and MBC value of (30 μM or 23.7 μg/mL) and (60 μM or 47.7 μg/mL) for *Staphylococcus aureus* and for *E. coli* (60 μM or 47.7 μg/mL) and (100 μM or 79 μg/mL), respectively. Moreover, PFBT-MI shows less cytotoxicity against mammalian cells at concentration greater than MIC.

INTRODUCTION

In the past few decades, there has been a substantial emergence of bacterial infections which has engrossed attention of researchers owing to their close association with human illness and food security. Moreover, extensive and irrational antibiotics use have resulted in the evolution of bacteria that are antibiotic resistant, posing acute threat to the global health. Growing resistance of microorganisms towards newly developed drugs is a serious concern that should be addressed rationally.[1-3] A recent report published by Center for Disease Control and Prevention (CDCP) states that the drug resistant bacteria affects the health of 2 million people annually and by 2050 antibiotic resistance would increase the average number of death to 10 million/year.[4]To address this globally precarious issue, efforts have been devoted by researchers worldwide to design probes with antimicrobial activity such as antibiotics, antimicrobial peptides, hydrogels, and inorganic nanoparticles. [5-14] Despite their individual effectiveness their clinical application remains elusive. Thus determined efforts are needed, to develop simple, sensitive, cost-effective techniques for bacterial identification and their killing to prevent the bacterial infections as well as outbreak of various epidemic diseases.

Fluorescence based methods have gained much attention in the field of life sciences and biomedicine and are widely employed for cancer theranostics,[15,16]inflammatory disorders,[17]and antibacterial treatments.[18,19] In recent years researchers have designed and used various fluorescent reporters for bacterial imaging and their killing such as nanomaterials (carbon nanotubes, carbon dots (CD),metal and metal oxides nanomaterials) and oligomers.[20] However, there are some challenges associated with them that avert its practical application.[21] For example, CD as a fluorescent probe at times, presents weak fluorescent signal, unclear and non-uniform bioimaging due to concentration dependent aggregation caused quenching (ACQ).[22] Similarly, the use of antibiotic capped nanomaterials (Ag, Au, ZnO, MgO, TiO, WS_2) may led to the growth of drug-resistant bacteria.[23] Recently, more advanced materials have been reported for bacterial identification, discrimination and killing such as aggregation-induced emission (AIE) luminogens[24-26], conjugated oligomers[27-

[29] and polymers.[30-33] Among them conjugated polymers are the attractive fluorescence probe for bacterial imaging and killing.

Conjugated polyelectrolytes (CPE's) are organic macromolecules with ionic side chains which endowing them with water solubility and facilitating numerous interactions towards innumerable chemical and biological analytes. CPE's have demonstrated their ability as outstanding class of materials in interdisciplinary areas such as optoelectronic devices, chemical, biological and medical science such as sensing, imaging, and theranostics because of their phenomenal attributes such as excellent photostability, high quantum efficiency, super sensitivity, amplified quenching effect and biocompatibility.[34-41] Recently, they have been explored as a novel light activated antibacterial material with remarkable activity in dark as well. In addition, water-soluble CPE's with cationic head group offers efficient targeting and binding on charged cell membrane of bacteria. Moreover, cationic CPEs act mainly by targeting and disintegrating the bacterial cell membrane via electrostatic attraction and insertion into the lipid membrane. As a result of this the bacterial cell membrane gets physically damaged and difficult to repair, therefore, restricting the potential development of bacterial resistance.[42-47] Remarkable advantages of using polymers with antibacterial property is their easily tailored structures and desired properties achieved by varying side chain cationic functionality and tuning badgap of the conjugated backbone. The former creates a difference in hydrophilic/hydrophobic interactions whereas the latter enhances singlet oxygen generation via increasing triplet state yield.[48]Schanze and co-workers reported a series of CPE's with different backbone structures and side chain functionalities for profound broad spectrum bacteria killing.[31,42,44,45,48,49] Similarly, Wang and co-workers develop a supramolecular approach based on cationic conjugated polymer for rapid discrimination and in-situ detection of pathogens.[50] However bacterial detection rely on change in emission intensity at single wavelength may results in the various interference such as autofluorescence, instrument fluctuation and environmental interventions. In this context, ratiometric technique such as Förster resonance energy transfer (FRET) offers more accurate results and self-calibration by exterminating various environmental and instrument factors thereby opening up a new avenue to design dual wavelength probes for real time bacteria monitoring in aqueous media with high sensitivity and low background signal.[51-53] Furthermore, imaging of bacteria without tedious wash free step forms an important component for success of antibacterial compounds. Wash free-imaging reduces the time as well as bacterial loss during bacterial imaging process.[24,54] Considering the above challenges

we designed a simple, cost effective, multifunctional approach for efficient bacterial detection in aqueous media, along with wash free bacterial imaging and also evaluated its antibacterial potential using conjugated polyelectrolyte with cationic head group.

Herein, we report a water-soluble CPE Poly[9,9-bis(6′-methyl imidazolium bromide)hexyl) fluorene-*co*-4,7-(2,1,3-benzothiadiazole)] (PFBT-MI) for bacterial imaging based on aggregation induced FRET and explored its antibacterial nature. Decorating the side chains with imidazolium group provided electrostatic binding sites on the negatively charged bacterial membrane. Taking advantage of FRET mechanism, the blue emitting CPE PFBT-MI displayed substantial color change from blue to yellow as well as changes in its photophysical properties after interaction with bacterial membrane via electrostatic and hydrophilic interaction which resulted in a very convenient wash free imaging of bacteria, at the same time demonstrating antibacterial activity as well. To the best of our knowledge, no FRET-based theranostic approach using single fluorophore for wash free imaging, and antibacterial activity has been reported to date.

EXPERIMENTAL SECTION

Material and instruments: PFBT-MI was synthesised according to previous literature.[55] All the reagents were procured from either Aldrich, Merck, or Ranbaxy (India). Nutrient broth (NB), brain–heart infusion (BHI), Luria–Bertani (LB), and bacterial growth medium were obtained from Himedia.

Characterisation: Absorption and emission studies were done on a Perkin Elmer Lambda-25 or JACSO V-630 and Horiba Fluoromax-4 spectrofluorometer, using quartz cuvettes (10 mm path length, slit width-3 nm at 298 K). Milli-Q water was used to prepare standard solutions. Fluorescence lifetime study was performed on Edinburgh Life Spec II instrument. DLS based size and charge measurement studies were performed on a Zeta sizer Nano ZS90, Model No. ZEN3690, Malvern instrument. Morphological changes before and after incubation of both the bacteria with PFBT-MI were observed with a Zeiss sigma FESEM at an accelerating voltage of 2 kV.

Imaging and detection of bacteria: For imaging, bacteria (10^8 CFU/mL) were treated with the polymer at the MIC concentration and incubated for 10min at 37 °C. After the treatment the bacteria was centrifuged for 1 min at 10000 rpm and dispersed in water. The samples were further drop casted on glass slides and sealed after mounting the cover slip. These

samples were then observed under a Zeiss LSM 880 confocal microscope (405 nm excitation).

The stock solution for detection consists of 1mM of PFBT-MI and was prepared in Milli-Q water. The bacteria (Gram-positive *Enterococcus faecalis* MTCC 439, *Staphylococcus aureus* MTCC 96, *Bacillus subtilis* MTCC 1305 and Gram-negative *Pseudomonas aeruginosa* MTCC 2488, *Escherichia Coli* MTCC 433, *Enterobacter aerogenes* MTCC 2822, *Escherichia Coli* DH5α) were serially diluted (10^{-1}, 10^{-2}, 10^{-3} and 10^{-4}) and the fluorescence spectra of PFBT-MI were monitored by adding 1mL each of above mentioned serially diluted bacterial suspensions into glass cuvette having (0.3μM) solution. *Bacillus subtilis*, *Pseudomonas aeruginosa*, *Escherichia Coli* 433 and *Enterobacter aerogenes* were grown in NB media, *Staphylococcus aureus*, *Enterococcus faecalis* was grown in BHI and *Escherichia Coli DH5α* was grown in LB (all at 37 °C for 12 h at 180 rpm)

Antibacterial activity: In order to carry out assessment of antibacterial activity Gram positive bacteria (*Enterococcus faecalis* MTCC 439, *Staphylococcus aureus* MTCC 96, *Bacillus subtilis* MTCC 1305) and Gram negative bacteria (*Pseudomonas aeruginosa* MTCC 2488, *Escherichia Coli* MTCC 433, *Enterobacter aerogenes* MTCC 2822, *Escherichia Coli* DH5α) were used. *Bacillus subtilis, Pseudomonas aeruginosa, Escherichia Coli 433 and Enterobacter aerogenes* were grown in NB media, *Staphylococcus aureus, Enterococcus faecalis* was grown in BHI and *Escherichia Coli* DH5α was grown in LB (all at 37 °C for 12 h at 180 rpm). The bacteria (10^8 CFU/mol) were treated with different concentrations of the polymer (0.01mMor 10μM to 0.2m Mor 200μM) for 12 hr. The minimum concentration wherein no visual turbidity is detected was considered as the MIC (minimum inhibitory concentration) value of the polymer. In order to determine the MBC (minimum bactericidal concentration), the treated bacterial cultures that did not show visual turbidity were re-inoculated in fresh media. MBC was taken as the minimum concentration that was bactericidal. The growth was checked by recording the OD at 595 nm using the UV-visible spectrophotometer.

FESEM Analysis:

Briefly, for FESEM analysis the bacteria were treated with MIC dose of the PFBT-MI for 6 h at 37 ºC followed by collection of the control and the treated bacteria by centrifugation. The samples were washed with sterile PBS twice and fixed in 2.5% glutaraldehyde (4 ºC for 90

min). The samples were then washed twice and finally suspended again in sterile MiliQ water. Thereafter, 5 μL from each sample was drop casted over a fresh aluminium foil covered glass slides and mounted on a metal stub with carbon tape and double coated with gold (Au). Finally the samples were analysed on a field emission scanning electron microscope (Zeiss Sigma 300) at 3.0 KV.

Protein leakage analysis: A standard Bradford assay was performed to analyse the protein leakage for both control and treated cells. In brief, *E.coli* and *S.aureus* cells were treated with MIC dose of polymer for 6 h at 37 °C. After centrifugation (15 min at 6000 rpm) the supernatant was collected and to 200 μL of each supernatant, 800 μL of the Bradford reagent was added. The optical density was measured at 595 nm after incubation in dark conditions for 10 min. Further, the absorbance of supernatants was measured at 280 nm for protein (before adding Bradford).[56]

Nucleic acid leakage analysis: In brief, *E.coli* and *S.aureus* cells were treated with MIC dose of polymer for 6 h at 37 °C. After centrifugation (6000 rpm for 15 min) the absorbance of the supernatant was recorded at 260 nm.[57]

Cell Culture: For cell culture studies HEK 293T (human embryonic kidney) cells were sourced from NCCS (National Centre for Cell Sciences), Pune, India. For culturing these cells, Dulbecco's modified Eagle's medium, supplemented with streptomycin (50 mg/mL), L-glutamine (4 mM), penicillin (50 units/mL), and 10% (v/v) fetal bovine serum (FBS; PAA Laboratories, Austria) was used and the cells were maintained at 37 °C in a 5% CO_2 incubator.

MTT Assay: For evaluation of the cell viability, 1×10^4 HEK cells were seeded in a 96-well plate and cultured overnight at 37 °C in a 5% CO_2 incubator. The cells were treated with various concentrations of PFBT-MI for 12 h, followed by 3-(4,5-dimethylthiazolyl-2)-2,5-diphenyltetrazolium bromide (MTT) assay. MTT is reduced by living cells (mitochondria) into a colored formazan product. Thereafter, the absorbance was recorded at 570 nm that related with the number of live or viable cells. The absorbance at 690 nm was subtracted by a background interference and the percentage of cell viability was calculated via the equation.

$$\% \text{ viable cell} = \frac{(\text{A570} - \text{A690})\text{of treated cells}}{(\text{A570} - \text{A690})\text{of control cells}} \times 100$$

RESULT AND DISCUSSION

The structure of Poly[9,9-bis(6′-methylimidazoliumbromide)hexyl)-fluorene-co-4,7-(2,1,3-benzothiadiazole)] (PFBT-MI) is illustrated in **Scheme 1.** The neutral conjugated polymer PFBT was synthesized via Suzuki cross coupling reaction using fluorene as the donor and incorporating 20 mol% of benzothiadiazole as acceptor. The PFBT was then post-functionalized with N-methylimidazole to obtain cationic conjugated polyelectrolyte PFBT-MI. The cationic imidazolium group endows PFBT-MI with good solubility in a polar solvent like water, dimethyl sulfoxide, methanol and helps in binding with the negatively charged bacterial membrane. The zeta potential value for PFBT-MI was found to be 15 mV (**Figure S1**). The PFBT-MI displays maximum absorption at 350nm and a weak band ranging from 415-530 nm characteristic of fluorene and benzothiadiazole unit respectively. The emission spectra of PFBT-MI exhibited a prominent fluorescence emission peak at 410 nm (ex. 350 nm) for fluorene unit (**Figure 1a**) and a weak emission band ranging from520-560nm (**Figure 1b**) corresponding to benzothiadiazole moiety, which indicates that PFBT-MI exhibits weak intra-chain FRET in dilute solution or non-aggregated state.

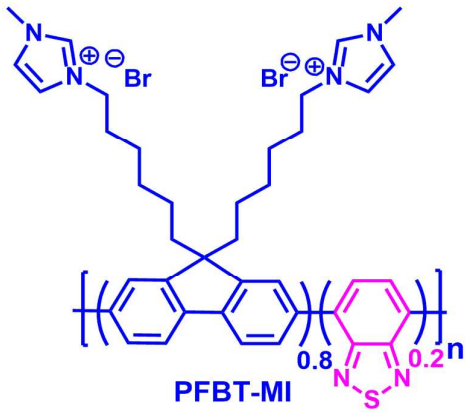

Scheme 1: Structure of Poly[9,9-bis(6′-methylimidazoliumbromide)hexyl)-fluorene-co-4,7-(2,1,3-benzothiadiazole)] (PFBT-MI).

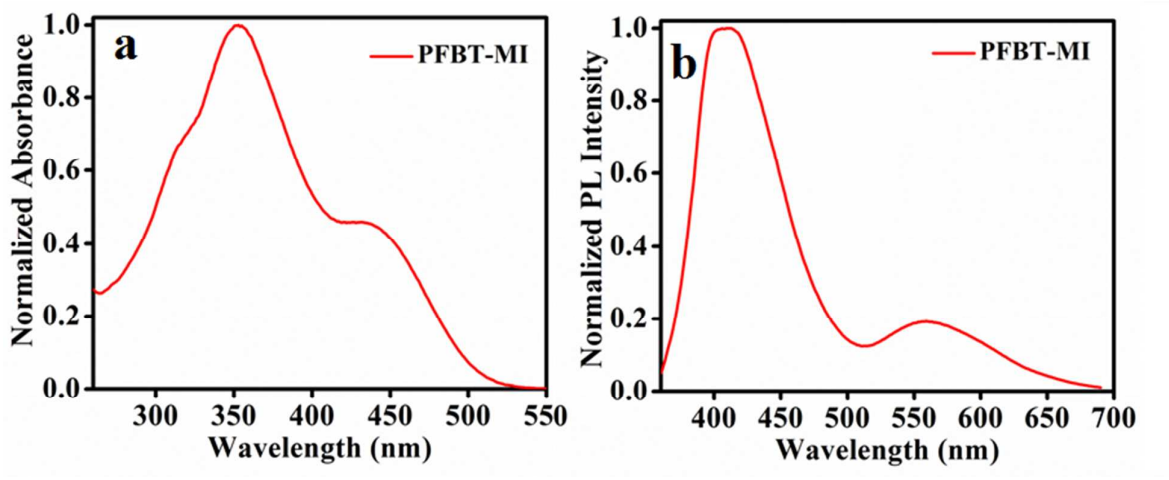

Figure 1: (a) UV-vis and **(b)** Fluorescence spectra of PFBT-MI in water.

The molecular state of PFBT-MI in water (good solvent) was studied by DLS that presents an observed distribution of ~12 nm which can be assigned to the hydrodynamic diameter of a single polymer chain. As the fraction of THF increases the polymer chain starts to form large aggregates (**FigureS2)**. This unimolecular state of polymer in water explains the presence of weak FRET efficiency from fluorene to the BT unit since inter-chain FRET is negligible as the molar ratio of the acceptor to donor moiety is low. The initial emission peak at 560 nm increases gradually on adding increasing fraction of THF (poor solvent) to the PFBT-MI in water (Figure 2a-b). Remarkably, the color of this solution got modified to yellow (from blue) in water and water-THF mixture respectively, realized clearly by the naked eye and under UV-light (lamp excitation-365 nm)(Inset of **Figure 2b**). The color change of PFBT-MI in water upon introducing the increasing fraction of THF indicates the appearance of an efficient inter-molecular FRET from fluorene (donor) to BT (acceptor) units of PFBT-MI due to polymeric chain's self-aggregation which increases the local concentration of BT units.

Furthermore, there is an overlapping spectral region between the emission of the donor (fluorene) and the acceptor (BT) absorption, a prerequisite for the phenomenon of FRET to occur (**Figure 3a**). To confirm the phenomenon of FRET, the lifetime of the conjugated polyelectrolyte in water and water-THF mixture was examined and the decay curves for PFBT-MI at 410 nm and 560 nm has been fitted mono-exponentially and bi-exponentially respectively (**Figure S3**). Upon exciting by a laser pulse of 375 nm, the decay monitored for PFBT-MI at 410 nm in pure water (0.743 ns) shows a reduction in the lifetime after introducing a fraction of THF (0.636ns) (**Figure 3b**). Whereas the average lifetime of PFBT-MI observed at 560 nm in water THF mixture (2.63 ns) increases as compared to the polymer

solution in pure water (0.29ns) (**Figure 3c**). Thus the above investigation explains the occurrence of FRET from fluorene unit to BT moiety with the help of aggregation induced by increasing the fraction of poor solvent into a good solvent.

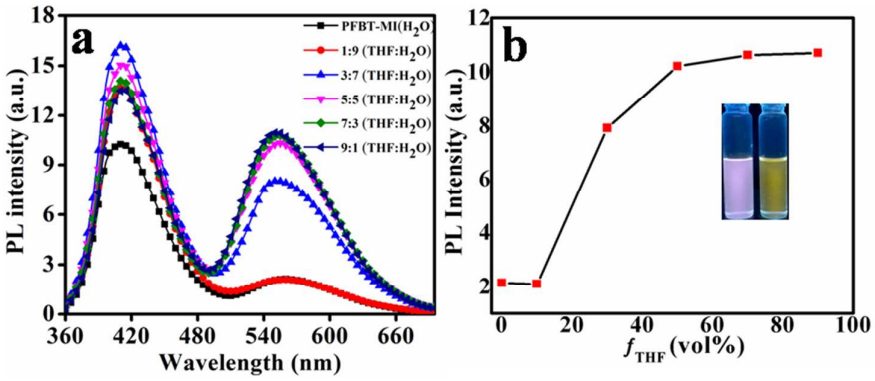

Figure 2: (a) Fluorescence emission spectra of PFBT-MI (10μM) with varying fraction of THF in water and **(b)** its corresponding plot showing the variation of emission intensity at 560 nm with increasing THF fractions. Inset: Color change of PFBT-MI in **(i)** water (blue) and **(ii)** water THF mixture (yellow).

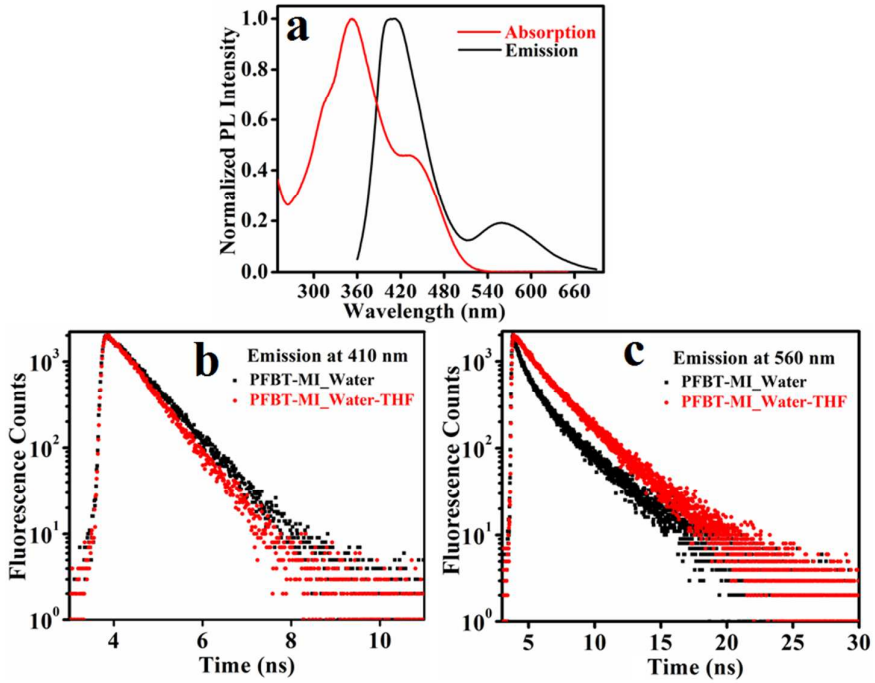

Figure 3: (a) Spectral overlap between emission of fluorene unit with the absorption of BT unit of PFBT-MI (10μM) in water. Time resolved photoluminescence of PFBT-MI (10μM) in water and water THF mixture observed at **(b)** 410 nm and **(c)** 560 nm using a laser excitation of 375 nm.

Imaging and Sensing of Bacteria

To check the practicability of PFBT-MI for visualization of bacteria live confocal laser scanning microscopy (CLSM) was performed (**Figure 4**). PFBT-MI successfully stained both Gram-positive bacteria and Gram-negative bacteria after incubation at MIC of PFBT-MI for 10 min. The unbound PFBT-MI does not emit in the yellow channel (560 nm) which, as a unique outcome, prominently eliminates the background emission while as the polymer chains get attached to the bacterial membrane, it turns on the bright yellow emission. Adhesion of PFBT-MI to the bacterial membrane via electrostatic interactions between the cationic PFBT-MI and the negatively charged bacterial surface as well as the lyophilic interactions between PFBT-MI backbone and lipid membrane of the bacteria increases the concentration of the polymer on the bacterial membrane. Consequently, the concentration of the acceptor moiety in the polymer around the donor units increase locally, which results in the efficient FRET from the fluorene (donor) to BT (acceptor) thus PFBT-MI emits in the yellow channel. Using this easy approach, the bacteria could be visualized without involving any washing process via the phenomenon of FRET thus, preventing loss of bacteria during washing and simplifying the process of imaging rapidly.

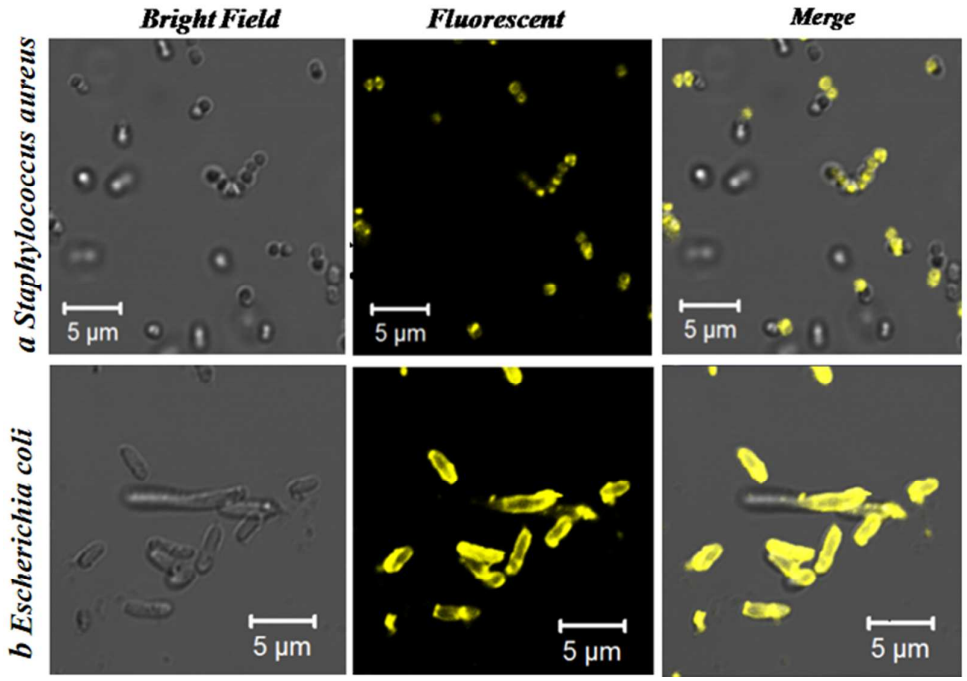

Figure 4: Confocal laser scanning fluorescence images (live) of **(a)** *Staphylococcus aureus* and **(b)** *Escherichia coli* after incubated with MIC of PFBT-MI for 10 min at 37°C. The fluorescence images were collected at 530-570 nm in confocal microscopy analysis.

To gain further insight into bacterial quantification fluorescence response of PFBT-MI with different bacterial strains was recorded in aqueous media. The fluorescence emission signals were measured by adding serially diluted bacterial suspension (1mL) into the glass cuvette containing PFBT-MI (0.3 μM) solution. Initially, PFBT-MI solution emits only at 410 nm (λ_{ex} 350 nm). Upon adding bacterial strains to PFBT-MI solution a new 560 nm peak appears and 410 nm peak diminishes reflecting the energy transfer process from donor fluorene to the acceptor BT unit. This shift in emission peak of PFBT-MI solution from 410 nm to 560 nm is evident from the color change of the polymer solution observed on irradiating UV-lamp (λ_{ex}-365 nm) upon adding bacteria as shown in **Figure 5a**. Furthermore, the FRET ratio I-Io/Io (where I= $I_{560}/I_{410}$for different bacterial strains and Io= I_{560}/I_{410} for the PFBT-MI only) of the polymer for different bacterial strain was calculated as shown in **Figure5b.**It was observed that different signal response was obtained with different strains of same bacterial species although having the same charge which may because of the reason that each strain possesses specific surface structures. This method thereby provides a simple, rapid technique for determining the presence of bacteria in a sample. The minimum concentration of bacteria that was able to shift the emission from blue to yellowish green is ~10^4 CFU/mL.

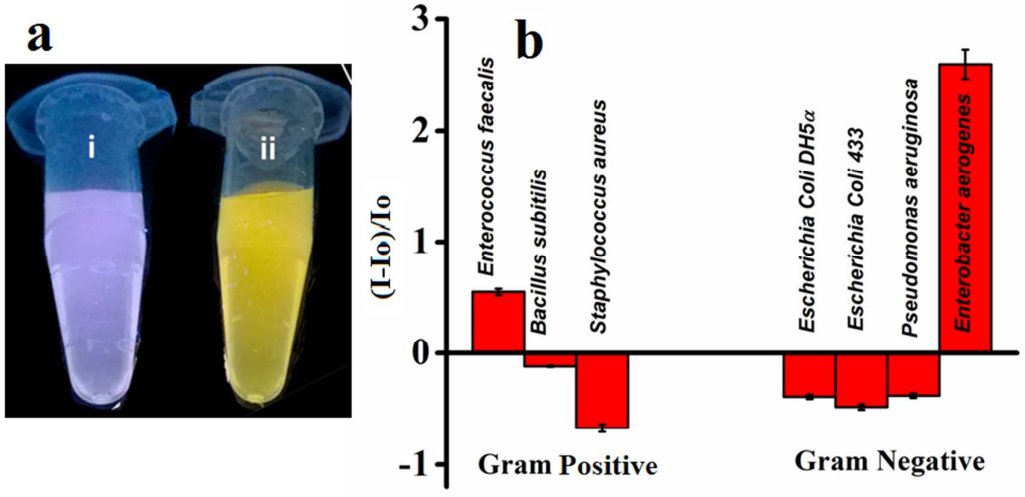

Figure 5: (a) Color of PFBT-MI (0.3 μM) solution from **(i)** blue to **(ii)** yellow upon adding bacterial strain (10^{-1}). **(b)** FRETratio of PFBT-MI (0.3 μM) with different bacterial strain.

Antibacterial Activity

The antibacterial activity of PFBT-MI was examined against both *Staphylococcus aureus* and *Escherichia coli* as representative Gram-positive and Gram-negative bacteria respectively.

The MIC and corresponding MBC value of polymer PFBT-MI for *Staphylococcus aureus* are (30µM or 23.7µg/mL) and (60µM or 47.7µg/mL) and for *E. Coli* are (60µM or47.7µg/mL) and (100µM or 79µg/mL), respectively. The growth curve was monitored up to 12 h. It was observed that the growth was inhibited at MIC concentration and no growth was observed in case of MBC (**Figure 6)**. Furthermore, when compared to earlier reports the observed MIC values for the antibacterial polymer in the present context are much lower (**Table S1)**.

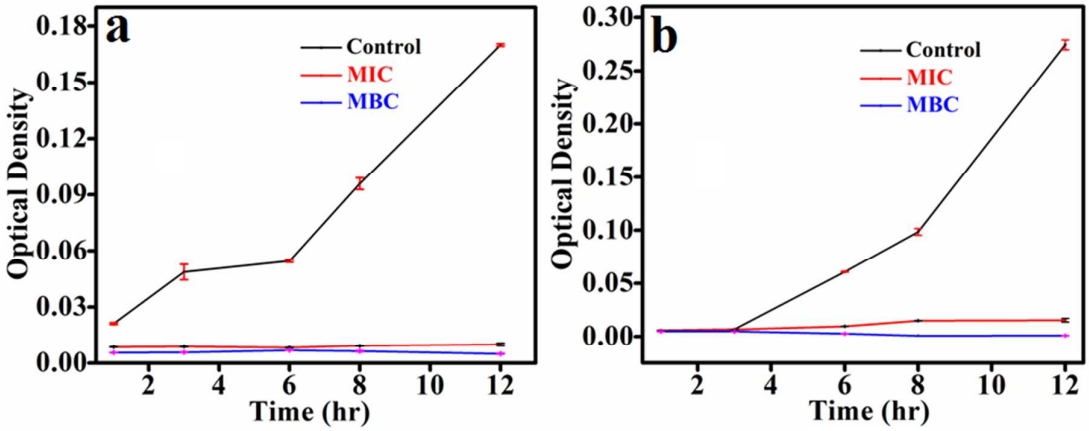

Figure 6: Growth curves of **(a)** *S.aureus* and **(b)** *E.coli* incubated with different concentration of PFBT-MI.

Table 1: MIC and MBC values of polymer PFBT-MI against *Staphylococcus aureus and Escherichia coli.*

Bacteria	**MIC (µg/mL)**	**MBC (µg/mL)**
Escherichia coli	47.7	79
Staphylococcus aureus	23.7	47.7

The values of MIC and MBC are slightly higher for Gram-negative *Escherichia coli* than Gram-positive *Staphylococcus aureus* **(Table 1)**. This heterogeneity could be due to difference in membrane structures of two species. The cell wall of Gram-positive bacteria has a porous thick layer of three dimensional cross linked peptidoglycan networks while Gram-negative has an additional outer membrane of lipopolysaccharide as well as thin peptidoglycan layer. The presence of auxiliary lipopolysaccharide layer complicates the binding and killing ability of PFBT-MI for Gram-negative *Escherichia coli*.

To validate the killing efficiency of PFBT-MI, plating experiment was performed. Control samples lacking PFBT-MI have dense bacterial growth as shown in **Figure S4**. The growth of *Staphylococcus aureus* and *Escherichia coli* are appreciably suppressed on treatment of these samples with polymer at respective MIC concentrations. However, at MBC concentrations of polymer, complete inhibition of bacterial growth is observed.

Mechanism of antibacterial activity

To investigate the mechanism of antibacterial activity of PFBT-MI, morphological changes of *Staphylococcus aureus* and *Escherichia coli* as models for Gram-positive and Gram-negative were examined before and after the treatment of conjugated polyelectrolyte by FESEM imaging at their respective MIC concentrations. For the control population of both, (*Escherichia coli* and of *Staphylococcus aureus)* the cell surface morphology appeared smooth and regular with clear edges that indicates a viable state of the bacteria. On the other hand in case of treated bacteria disintegration of the cell membrane was observed. It was concluded from FESEM results that PFBT-MI successfully caused bacterial cell death by disruption of the cell membrane as shown in **Figure 7 & Figure 8.** It has been previously reported that imidazolium molecules and polymers can have antibacterial activity towards both Gram-positive and Gram-negative bacteria.[49,58,59] Therefore, due to the cationic nature of PFBT-MI, it can possibly interact with the negative cell membrane of the bacteria thereby leading to disruption of the membrane and leakage of intracellular constituents as presented in the schematic of **Figure 9**.

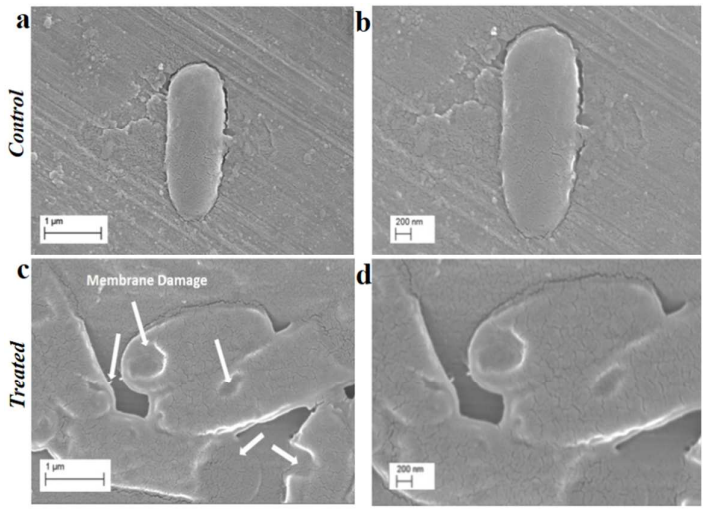

Figure 7: FESEM images of *E.coli* (a-b) and *E.coli* (c-d) incubation without and with PFBT-MI respectively.

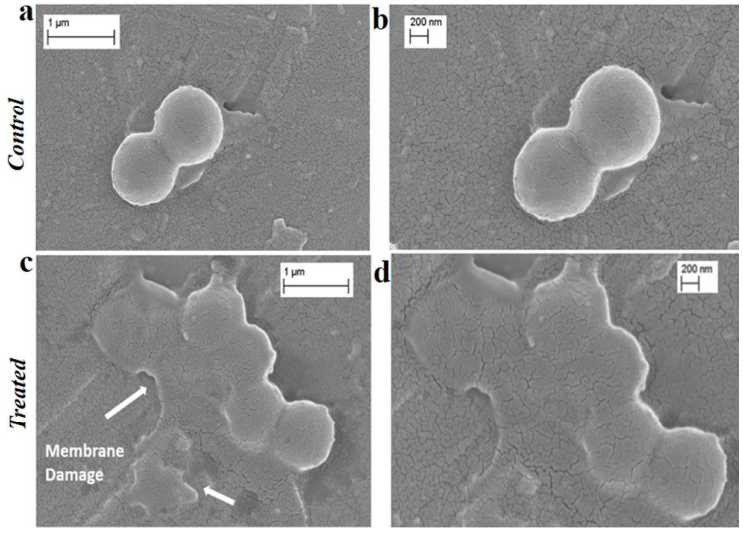

Figure 8: FESEM images of control *S.aureus* (a,b) and treated *S. aureus* (c,d) incubation without and with PFBT-MI respectively.

To gain additional insight on mechanism of bacterial killing protein and nucleic acid leakage studies has been carried out. In the protein leakage study both Bradford (Figure S7) as well as OD measurement at 280 nm suggested that there was an increased amount of protein present in the supernatant of the treated cells signifying membrane damage due to which proteins are released in the supernatant. Also the nucleic acid leakage analysis showed increased OD at 260 nm in case of the treated cells indicating likely release of nucleic acid into the supernatant due to the damage of the membrane (Figure S8). This data corroborates with the FESEM analysis which also suggested bacterial cell death due to membrane disruption.

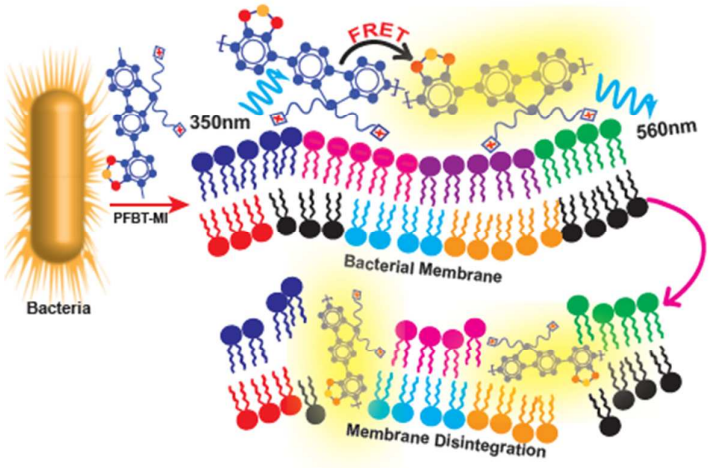

Figure 9: Proposed schematic representation of bacterial membrane with PFBT-MI and its antibacterial activity.

Cytotoxicity results

The use of antibacterial agents for biomedical application is gaining interest, as they selectively kill the pathogenic bacteria over mammalian cells. Thus, they can be applied as an antibacterial coating or bactericidal surface for medical devices. In this regard, the cytotoxicity nature of PFBT-MI was examined by MTT assay. The cell viability assay of PBFT-MI shows that approximately 80% of the cells were viable at the 100μM concentration (which is the maximum dose used in antibacterial studies) after 12 h of treatment (Figure S9). This indicates that the polymer PFBT-MI is less toxic in nature towards mammalian cells and shows pronounced killing activity towards bacterial cells (Gram-positive and Gram-negative).

CONCLUSION

In summary, we have developed and explored the potential application of cationic conjugated polyelectrolyte PFBT-MI in wash free bacterial imaging as well as its antibacterial activity. The side chain strapped imidazolium group of PFBT-MI makes the solution phase quantification and imaging process simple. The imaging process is wash free as the PFBT-MI underwent aggregation induced FRET from fluorene unit to the BT on binding with the negatively charged bacterial surface. The PFBT-MI exhibited effective antibacterial activity against *Staphylococcus aureus* (Gram-positive) and *Escherichia coli* (Gram-negative) bacteria. The killing efficacy was higher for *Staphylococcus aureus* bacteria compared to *Escherichia coli*. The MIC value for Gram-positive and Gram-negative bacteria were 23.7μg/mL and 47.7μg/mL respectively. The antibacterial action of PFBT-MI was due to the disintegration of the bacterial cell membrane that resulted in leakage of all the intracellular constituents and ultimately cell death. This conclusion was well supported by FESEM analysis as well as by performing protein and nucleic acid leakage studies.

ASSOCIATED CONTENT

Supporting Information: Zeta potential graph of PFBT-MI, aggregation studies, life time fitting plots, cell plating studies, Protein and Nucleic acid leakage study, Cytotoxicity assay. This material is available free of charge via the Internet at http://pubs.acs.org.

AUTHOR INFORMATION

Corresponding Author

***E-mail:** pki@iitg.ac.in **FAX:** +91 361 258 2349

Notes

The authors declare no competing financial interest.

ACKNOWLEDGEMENT

Financial grants from Department of Information Technology, DeitY Project no. 5(9)/2012-NANO (Vol.II), Department of Science and Technology (DST), India (Nos. DST/TSG/PT/2009/23 and DST/SERB/EMR/2014/000034), DST-Max Planck Society, Germany (IGSTC/MPG/PG(PKI)/2011A/48) are gratefully acknowledged. The CIF and Department of Chemistry, IIT Guwahati and DBT program support facility, are acknowledged for instrument facilities.

REFERENCE

[1] Ivnitski, D.; Abdel-Hamid, I.; Atanasov, P.; Wilkins, E. D. Biosensors for Detection of Pathogenic Bacteria. *Biosens. Bioelectron.***1999**, *14*, 599–624.

[2] Daszak, P., Cunningham, A. A.; Hyatt, A. D. Emerging Infectious Diseases of Wildlife Threats to Biodiversity and Human Health. *Science* **2000**, *287*, 443–449.

[3] Hoffmann, J. A.; Kafatos, F. C.; Janeway, C. A.; Ezekowitz, R. Phylogenetic Perspectives in Innate Immunity. *Science* **1999**, *284*, 1313–1318.

[4] Mendoza, G.; Regiel-Futyra, A.; Andreu, V.; Sebastian, V.; Kyzioł, A.; Stochel, G.; Arruebo, M. Bactericidal Effect of Gold−Chitosan Nanocomposites in Coculture Models of Pathogenic Bacteria and Human Macrophages. ACS *Appl. Mater. Interfaces* **2017**, *9*, 17693–17701.

[5] Li, Q.; Wu, Y.; Lu, H.; Wu, X.; Chen, X.; Song, N.; Yang, Y.-W.; Gao, H. Construction of Supramolecular Nanoassembly for Responsive Bacterial Elimination and Effective Bacterial Detection. *ACS Appl. Mater. Interfaces* **2017**, *9*, 10180−10189.

[6] Liu, L.; Xu, K.; Wang, H.; Tan, P. J.; Fan, W.; Venkatraman, S. S.; Li, L.; Yang, Y.-Y. Self-Assembled Cationic Peptide Nanoparticles as an Efficient Antimicrobial Agent. *Nat. Nanotechnol***. 2009**, *4*, 457−463.

[7] Irwansyah, I. ; Li , Y-Q.; Shi , W.; Qi, D.; Leow, W. R.; Tang, M. B. Y.; Li, S.; Chen, X. Gram-Positive Antimicrobial Activity of Amino Acid-Based Hydrogels. *Adv. Mater.* **2015**, *27*, 648–654.

[8] Chen, J.; Wang, F.; Liu, Q.; Du, J. Antibacterial Polymeric Nanostructures for Biomedical Applications. *Chem. Commun.* **2014**, *50*, 14482–14493.

[9] Guilhelmelli, F.; Vilela, N.; Albuquerque, P.; Derengowski, L. S.; Silva-Pereira, I.; Kyaw, C. M. Antibiotic Development Challenges: the Various Mechanisms of Action of Antimicrobial Peptides and of Bacterial Resistance. *Front. Microbiol.* **2013**, *4*, 353–365.

[10] Fernandez-Lopez, S.; Kim, H.-S.; Choi, E. C.; Delgado, M.; Granja, J. R.; Khasanov, A.; Kraehenbuehl, K.; Long, G.; Weinberger, D. A.; Wilcoxen, K. M.; Ghadiri, M. R. Antibacterial Agents Based on the Cyclic D, L-A-Peptide Architecture. *Nature* **2001**, *412*, 452−455.

[11] Yeaman, M. R.; Yount, N. Y. Mechanisms of Antimicrobial Peptide Action and Resistance. *Pharmacol Rev* **2003**, *55*, 27−55.

[12] Kenawy, E.-R.; Worley, S. D.; Broughton, R. The Chemistry and Applications of Antimicrobial Polymers: A State-of-the-Art Review. *Biomacromolecules* **2007**, *8*, 1359−1384.

[13] Brogden, K. A. Antimicrobial Peptides: Pore Formers or Metabolic Inhibitors in Bacteria? *Nat. Rev. Microbiol.* **2005**, *3*, 238−250.

[14] Zhou, C.; Wang, F.; Chen, H.; Li, M.; Qiao, F.; Liu, Z.; Hou, Y.; Wu, C.; Fan, Y.; Liu, L.;Wang, S.; Wang, Y.; Selective Antimicrobial Activities and Action Mechanism of Micelles Self-Assembled by Cationic Oligomeric Surfactants. *ACS Appl. Mater. Interfaces* **2016**, *8*, 4242−4249.

[15] Gui, C.; Zhao, E.; Kwok, R. T. K.; Leung, A. C. S.; Lam, J. W. Y.; Jiang, M.; Deng, H.; Cai, Y.; Zhang, W.; Sub, H.; Tang, B. Z.; AIE-active Theranostic System: Selective Staining and Killing of Cancer Cells. *Chem. Sci.* **2017**, *8*, 1822.

[16] Qian, C.; Yu , J.; Chen , Y.; Hub, Q.; Xiao, X.; Sun, W.; Wang, C.; Feng, P.; Shen, Q.-D.; Gu, Z. Light-Activated Hypoxia-Responsive Nanocarriers for Enhanced Anticancer Therapy. *Adv. Mater.* **2016**, *28*, 3313–3320.

[17] Sakamoto, F. H.; Torezan, L.; Anderson, R. R. Photodynamic Therapy for Acne Vulgaris: a Critical Review from Basics to Clinical Practice: Part II. Understanding

Parameters for Acne Treatment with Photodynamic Therapy. *J. Am. Acad. Dermatol*. **2010**, *63*,195–211.

[18] Riduan, S. N.; Zhang, Y. G. Imidazolium Salts and Their Polymeric Materials for Biological Applications. *Chem. Soc. Rev.* **2013**, *42*, 9055−9070.

[19] Li, J.; Zhao, Q.; Shi, F.; Liu, C.; Tang, Y. NIR-Mediated Nanohybrids of Upconversion Nanophosphors and Fluorescent Conjugated Polymers for High-Efficiency Antibacterial Performance Based on Fluorescence Resonance Energy Transfer. *Adv. Healthcare Mater.* **2016**, *23*, 2967–2971.

[20] Liu, G-J.; Tian, S.-N.; Li, C.-Y.; Xing, G.-W.; Zhou, L. Aggregation-Induced-Emission Materials with Different Electric Charges as an Artificial Tongue: Design, Construction, and Assembly with Various Pathogenic Bacteria for Effective Bacterial Imaging and Discrimination. *ACS Appl. Mater. Interfaces* **2017**, *9*, 28331−28338.

[21] Dutta, D.; Sailapu, S. K.; Chattopadhyay, A.; Ghosh, S. S. Phenylboronic Acid Templated Gold Nanoclusters for Mucin Detection Using a Smartphone-Based Device and Targeted Cancer Cell Theranostics. *ACS Appl. Mater. Interfaces* **2018**, *10*, 3210−3218.

[22] Zhang, Y.; Li, C.; Fan, Y.; Wang, C.; Yang, R.; Liu, X.; Zhou, L. A Self-quenching-Resistant Carbon Nanodot Powder with Multicolored Solid-State Fluorescence for Ultra-fast Staining of Various Representative Bacterial Species within One Minute. *Nanoscale* **2016**, *8*, 19744–19753.

[23] Jiang, Y.-W.; Gao, G.; Zhang, X.; Jia, H.-R.; Wu, F.-G. Antimicrobial Carbon Nanospheres. *Nanoscale* **2017**, *9*, 15786–15795.

[24] Zhao, E.; Chen, Y.; Chen, S.; Deng, H.; Gui, C.; Leung, C. W.; Hong, Y.; Lam, J. W.; Tang, B. Z. A Luminogen with Aggregation Induced Emission Characteristics for Wash-Free Bacterial Imaging, High-Throughput Antibiotics Screening and Bacterial Susceptibility Evaluation. *Adv. Mater.* **2015**, *27*, 493–4937.

[25] Zhao, E.; Chen, Y.; Wang, H.; Chen, S.; Lam, J.W. Y.; Leung, C.W. T.; Hong, Y.; Tang, B.Z. Light-Enhanced Bacterial Killing and Wash-Free Imaging Based on AIE Fluorogen. *ACS Appl. Mater. Interfaces* **2015**, *7*, 7180−7188.

[26] Feng, G.; Yuan, Y.; Fang, H.; Zhang, R.; Xing, B.; Zhang, G.; Zhang, D.; Liu, B. A Light-up Probe with Aggregation-induced Emission Characteristics (AIE) for Selective Imaging, Naked-eye Detection and Photodynamic Killing of Gram-positive Bacteria. *Chem. Commun.* **2015**, *51*, 12490–12493.

[27] Thomas, A.W.; Catania, C.; Garner, L.E.; Bazan, G.C. Pendant Ionic Groups of Conjugated Oligoelectrolytes Govern their Ability to Intercalate into Microbial Membranes. *Chem. Commun.* **2015**, *51*, 9294—9297.

[28] Yan, H.; Rengert, Z.D.; Thomas, A.W.; Rehermann, C.; Hinks, J.; Bazan, G.C. Influence of Molecular Structure on the Antimicrobial Function of Phenylenevinylene Conjugated Oligoelectrolytes. *Chem. Sci.* **2016**, *7*, 5714–5722.

[29] Wang, B.; Wang, M.; Mikhailovsky, A.; Wang, S.; Bazan, G.C. A Membrane-Intercalating Conjugated Oligoelectrolyte with High-Efficiency Photodynamic Antimicrobial Activity. *Angew. Chem. Int. Ed.* **2017**, *56*, 5031–5034.

[30] Chen, H.; Li, M.; Liu, Z.; Hu, R.; Li, S.; Guo, Y.; Lv, F.; Liu, L.; Wang, Y.; Yi, Y.; Wang, S. Design of Antibacterial Peptide-like Conjugated Molecule with Broad Spectrum Antimicrobial Ability. *Sci. China Chem.* **2018**, *61*, 113-117.

[31] Ji, E.; Parthasarathy, A.; Corbitt, T.S.; Schanze, K.S.; Whitten, D.G. Antibacterial Activity of Conjugated Polyelectrolytes with Variable Chain Length. *Langmiur* **2011**, *27*, 10763–10769.

[32] Yang, Y.; Cai1, Z.; Huang, Z.; Tang, X.; Zhang, X. Antimicrobial Cationic Polymers: from Structural Design to Functional Control. *Polymer* **2018**, *50*, 33–44.

[33] Konai, M.M.; Bhattacharjee, B.; Ghosh, S.; Haldar, J. Recent Progress in Polymer Research to Tackle Infections and Antimicrobial Resistance. *Biomacromolecules* **2018**, *19*, 1888−1917.

[34] Henson, Z. B.; Zhang, Y.; Nguyen, T.-Q.; Seo, J. H.; Bazan, G. C. Synthesis and Properties of Two Cationic Narrow Band Gap Conjugated Polyelectrolytes. *J. Am. Chem. Soc.* **2013**, *135*, 4163–4166.

[35] Gaylord, B. S.; Heeger, A. J.; Bazan, G. C. DNA Hybridization Detection with Water-Soluble Conjugated Polymers and Chromophore-Labeled Single-Stranded DNA. *J. Am. Chem. Soc.* **2003**, *125*, 896–900.

[36] Liu, B.; Bazan, G. C. Homogeneous Fluorescence-Based DNA Detection with Water-Soluble Conjugated Polymers. *Chem. Mater.* **2004**, *16*, 4467–4476.

[37] Thomas, S. W., III; Joly, G. D.; Swager, T. M. Chemical Sensors Based on Amplifying Fluorescent Conjugated Polymers. *Chem. Rev.* **2007**, *107*, 1339–1386.

[38] Ho, H. A.; Najari, A.; Leclerc, M. Optical Detection of DNA and Proteins with Cationic Polythiophenes. *Acc. Chem. Res.* **2008**, *41*, 168–178.

[39] Zhu, C.; Liu, L.; Yang, Q.; Lv, F.; Wang, S. Water-Soluble Conjugated Polymers for Imaging, Diagnosis, and Therapy. *Chem. Rev.* **2012**, *112*, 4687–4735.

[40] McQuade, D. T.; Pullen, A. E.; Swager, T. M. Conjugated Polymer-Based Chemical Sensors. *Chem. Rev.* **2000**, *100*, 2537–2574.

[41] Liang, J.; Li, K.; Liu, B. Visual Sensing with Conjugated Polyelectrolytes. *Chem. Sci.* **2013**, *4*, 1377–1394.

[42] Wang, Y.; Jett, S. D.; Crum, J.; Schanze, K. S.; Chi, E. Y.; Whitten D. G. Understanding the Dark and Light-Enhanced Bactericidal Action of Cationic Conjugated Polyelectrolytes and Oligomers. *Langmuir* **2013**, *29*, 781–792.

[43] Zhou, C.; Wang, F.; Chen, H.; Li, M.; Qiao, F.; Liu, Z.; Hou, Y.; Wu, C.; Fan, Y.; Liu, L.; Wang, S.; Wang, Y. Selective Antimicrobial Activities and Action Mechanism of Micelles Self-Assembled by Cationic Oligomeric Surfactants. *ACS Appl. Mater. Interfaces* **2016**, *8*, 4242–4249.

[44] Wang Y.; Zhou Z.; Zhu J.; Tang Y.; Canady T. D.; Chi E. Y.; Schanze K. S.; Whitten D.G. Dark Antimicrobial Mechanisms of Cationic Phenylene Ethynylene Polymers and Oligomers against Escherichia coli. *Polymers* **2011**, *3*, 1199–1214.

[45] Wang, Y.; Corbitt, T. S.; Jett, S. D.; Tang, Y.; Schanze, K. S.; Chi, E. Y.; Whitten, D. G. Direct Visualization of Bactericidal Action of Cationic Conjugated Polyelectrolytes and Oligomers. *Langmuir* **2012**, *28*, 65−70.

[46] Sun, H.; Yin, B.; Ma, H.; Yuan, H.; Fu, B.; Liu. L. Synthesis of a Novel Quinoline Skeleton Introduced Cationic Polyfluorene Derivative for Multimodal Antimicrobial Application. *ACS Appl. Mater. Interfaces* **2015**, *7*, 25390−25395.

[47] Kenawy, El-R.; Worley, S. D.; Broughton, R. The Chemistry and Applications of Antimicrobial Polymers: A State-of-the-Art Review. *Biomacromolecules* **2007**, *8*, 1359−1384.

[48] Ji, E.; Corbitt, T. S.; Parthasarathy, A.; Schanze, K. S.; Whitten, D. G. Light and Dark-Activated Biocidal Activity of Conjugated Polyelectrolytes. *ACS Appl. Mater. Interfaces* **2011**, *3*, 2820–2829.

[49] Parthasarathy, A.; Pappas, H. C.; Hill, E. H. ; Huang, Y.; Whitten, D. G.; Schanze K. S. Conjugated Polyelectrolytes with Imidazolium Solubilizing Groups. Properties and Application to Photodynamic Inactivation of Bacteria. *ACS Appl. Mater. Interfaces* **2015**, *7*, 28027–28034.

[50] Bai, H.; Chen, H.; Hu, R.; Li, M.; Lv, F.; Liu, L., Wang, S. Supramolecular Conjugated Polymer Materials for in Situ Pathogen Detection. *ACS Appl. Mater. Interfaces* **2016**, *8*, 31550−31557.

[51] Jares-Erijman, E. A.; Jovin, T. M. FRET Imaging. *Nat. Biotechnol.* **2003**, *21*, 1387–1395.

[52] Varghese, S. S; Zhu, .Y.; Davis, T. J.; Trowell, S. C. FRET for Lab-on-a-chip Devices — Current Trends and Future Prospects. *Lab Chip* **2010**, *10*, 1355–1364.

[53] Hussain, S.; Malik, A. H.; Iyer, P. K. FRET-assisted Selective Detection of Flavins via Cationic Conjugated Polyelectrolyte under Physiological Conditions. *J. Mater. Chem. B* **2016**, *4*, 4439–4446.

[54] Shi, X.; Yu, C.Y. Y.; Su, H.; Kwok, R. T. K.; Jiang, M.; He, Z.; Lam, J. W. Y.; Tang, B. Z. A Red-Emissive Antibody–AIEgen Conjugate for Turn-on and Wash-free Imaging of Specific Cancer Cells. *Chem. Sci.* **2017***, 8, 7014–7024.*

[55] Malik A. H.; Hussain S.; Iyer, P. K. Aggregation-Induced FRET via Polymer−Surfactant Complexation: A New Strategy for the Detection of Spermine. *Anal. Chem.* **2016**, *88*, 7358–7364.

[56] Nanda, S. S.; Yi, D. K.; Kim, K. Study of antibacterial mechanism of Graphene Oxide using Raman Spectroscopy. *Sci. Rep.* **2016**, *6,* 28443.

[57] Reddy, L. S.; Nisha, M. M.; Joice, M.; Shilpa, P. N. Antimicrobial Activity of Zinc Oxide (ZnO) Nanoparticle Against Klebsiella pneumonia. *Pharm. Biol.*, **2014**, *52*, 1388-1397.

[58] Liu, L. H.; Huang, Y.; Riduan, S. N.; Gao, S. J.; Yang, Y. Y.; Fan, W. M.; Zhang, Y. G. Main-Chain Imidazolium Oligomer Material as a Selective Biomimetic Antimicrobial Agent. *Biomaterials* **2012**, *33*, 8625−8631.

[59] Riduan, S. N.; Zhang, Y. G. Imidazolium Salts and Their Polymeric Materials for Biological Applications. *Chem. Soc. Rev.* **2013**, *42*, 9055−9070.

Table of Contents